DMD Fast Forward. Published on February 5, 2009 as doi:10.1124/dmd.108.026112



# Utility of *MetaSite* in Improving Metabolic Stability of the Neutral Indomethacin Amide Derivative and Selective Cyclooxygenase-2 (COX-2) Inhibitor 2-(1-(4-Chlorobenzoyl)-5-methoxy-2-methyl-1*H*-indol-3-yl]-*N*-phenethyl-acetamide

David Boyer, Jonathan N. Bauman, Daniel P. Walker, Brendon Kapinos, Kapil Karki, and Amit S. Kalgutkar

Pharmacokinetics, Dynamics and Metabolism Department and Discovery Chemistry, Pfizer Global Research and Development, Groton, Connecticut (D.B., J.N.B., B.K., K.K., A.S.K.) and Discovery Chemistry, Pfizer Global Research and Development, St. Louis Laboratories, Chesterfield, Missouri (D.P.W.)

DMD Fast Forward. Published on February 5, 2009 as DOI: 10.1124/dmd.108.026112
This article has not been copyedited and formatted. The final version may differ from this version.


Running Title: Metabolic Stability of Indomethacin-Amide-based COX-2 Inhibitors

Number of Text Pages: (including references) 22

Number of Tables: 3

Number of Figures: 8

Number of References: 19

Number of Words in Abstract: 243

Number of Words in Introduction: 665

Number of Words in Discussion: 1482

Abbreviations used are: P450, cytochrome P450; NSAID, nonsteroidal anti-inflammatory agent; $t_{1/2}$, half-life; iv, intravenous; po, oral; LC-MS/MS, liquid chromatography tandem mass spectrometry; MRM, multiple reaction monitoring, CID, collision-induced dissociation.

**Correspondence should be addressed to:** Amit S. Kalgutkar, Pharmacokinetics, Dynamics, and Metabolism Department, Pfizer Global Research and Development, Groton, CT 06340. Phone: (860)-715-2433. E-mail: amit.kalgutkar@pfizer.com

DMD Fast Forward. Published on February 5, 2009 as DOI: 10.1124/dmd.108.026112
This article has not been copyedited and formatted. The final version may differ from this version.


**Abstract**

Prediction of the metabolic sites for new compounds, synthesized or virtual, is important in the rational design of compounds with increased resistance to metabolism. The aim of the present investigation was to use rational design together with *MetaSite*, an *in silico* tool for predicting metabolic soft spots, to synthesize compounds that retain their pharmacological effects but are metabolically more stable in the presence of P450 enzymes. The model compound for these studies was the phenethyl amide (**1**) derivative of the nonsteroidal anti-inflammatory drug (NSAID) indomethacin. Unlike the parent NSAID, **1** is a potent and selective cyclooxygenase-2 inhibitor and non-ulcerogenic anti-inflammatory agent in the rat. This pharmacologic benefit is offset by the finding that **1** is very unstable in rat and human microsomes due to extensive P4503A4/2D6-mediated metabolism on the phenethyl group, experimental observations that were accurately predicted by *MetaSite*. The information was used to design analogs with polar (glycinyl) and/or electron-deficient (fluorophenyl-, fluoropyridinyl) amide substituents to reduce metabolism in **1**. *MetaSite* correctly predicted the metabolic shift from oxidation on the amide substituent to *O*-demethylation for these compounds, while rat and human microsomal stability studies and pharmacokinetic assessments in the rat confirmed that the design tactics for improving pharmacokinetic attributes of **1** had worked in our favor. In addition, the fluorophenyl- and pyridinyl amide derivatives retained the potent and selective COX-2 inhibition demonstrated with **1**. Overall, the predictions from *MetaSite* gave useful information leading to the design of new compounds with improved metabolic properties.

DMD Fast Forward. Published on February 5, 2009 as DOI: 10.1124/dmd.108.026112
This article has not been copyedited and formatted. The final version may differ from this version.


## Introduction

In the early drug discovery phase, many compounds suffer from high oxidative metabolic instability mediated by cytochrome P450 (P450s) enzymes, which often results in poor oral pharmacokinetics in preclinical species. While high-throughput *in vitro* microsomal assays that monitor metabolic stability provide a convenient means for "rank-ordering" large numbers of compounds, information pertaining to identification of "soft spots" for unstable compounds cannot be discerned from such analyses and requires separate metabolite identification studies. Unlike microsomal stability assays, metabolite identification experiments are low-throughput and cannot keep pace with high speed chemistry efforts. In addition, there are scenarios where metabolism studies will limit the labile site(s) to a certain region within the molecule. To guide chemists in the "right direction", information on the exact metabolic site is often preferred. Therefore, in addition to existing *in vitro* assays, a value added proposition would be the use of *in silico* tools to precisely predict regiochemistry of metabolism for compounds (synthesized or only virtual); information which could be used towards rational design of pharmacologically active compounds with improved metabolic properties.

*MetaSite* is an *in silico* tool that can identify the most likely sites of P450-mediated oxidative metabolism in a compound (Cruciani et al., 2005) and has seen some success in *de novo* design of pharmacologic compounds with improved metabolic properties (Ahlstrom et al., 2007). *MetaSite* is based on two factors: chemical reactivity of the substrate and enzyme-substrate similarity analysis. *MetaSite* performs a similarity analysis of the protein-cavity interaction profile and the potential substrate. The chemical reactivity of fragments toward oxidation, representing the activation energy of the conversion of substrate to metabolite, is precomputed and stored within the program. Consequently, if the similarity search gives a high score for a fragment, the chemical reactivity of that fragment is included in the final "hot spot" prediction (Cruciani et al., 2005; Zamora et al., 2003).

In this paper, we have explored the performance of *MetaSite* as a tool to guide drug discovery efforts where prior information on metabolic fate does not exist. For this endeavor, we chose a series of

DMD Fast Forward. Published on February 5, 2009 as DOI: 10.1124/dmd.108.026112
This article has not been copyedited and formatted. The final version may differ from this version.


selective cyclooxygenase-2 (COX-2) inhibitors comprising of neutral amide derivatives of the nonsteroidal anti-inflammatory drug (NSAID) indomethacin as target compounds for optimization (Figure 1) (Kalgutkar et al., 2000a; Kalgutkar et al., 2000b). Indomethacin is a non-selective inhibitor of the COX isozymes COX-1 and COX-2, but derivatization of its carboxylic acid group to ester or amide analogs produces compounds that are highly selective and potent COX-2 inhibitors. 2-(1-(4-Chlorobenzoyl)-5-methoxy-2-methyl-1*H*-indol-3-yl]-*N*-phenethyl-acetamide (**1**) (see Figure 1) is a prototypical compound (> 1000-fold COX-2 selectivity) in the series that demonstrates *in vivo* anti-inflammatory activity comparable to indomethacin but is devoid of the ulcerogenic effects associated with the parent NSAID (Kalgutkar et al., 2000a). The attractive pharmacologic and safety advantage of **1** over indomethacin, however, is offset by the metabolic instability of **1** in rat and human liver microsomes (half-life ($t_{1/2}$) < 5 min) when compared with indomethacin ($t_{1/2}$ > 60 min) (Remmel et al., 2004; Obach et al., 2008). Consistent with the *in vitro* finding, **1** exhibited a very short $t_{1/2}$ (< 20 min) upon intravenous administration to rats (Remmel et al., 2004). *In vitro* metabolism studies in human liver microsomes identified oxidations on the pendant phenethyl substituent by P4503A4 and *O*-demethylation by P4502D6 as the principal metabolic routes (Remmel et al., 2004).

In the first set of experiments, we used *MetaSite* retrospectively to predict P450-derived metabolites of **1** and indomethacin (for comparative purposes). Predictions were then compared with experimental data. Next, we applied *MetaSite* to predict metabolites for *virtual* indomethacin-amides (Figure 2) for which no prior knowledge existed on their metabolic fate. In this exercise, appropriate structural modifications were included in the virtual structures to reduce P450 metabolism. The virtual compounds were synthesized and experimental *in vitro* metabolism data (compound stability, metabolite identification and P450 phenotyping) was generated on the analogs. The synthesized compounds along with **1** were administered to rats to examine whether the structural changes afforded overall improvements in clearance. The collective findings of these analyses are summarized, herein.

## Materials and Methods

DMD Fast Forward. Published on February 5, 2009 as DOI: 10.1124/dmd.108.026112
This article has not been copyedited and formatted. The final version may differ from this version.


**Materials.** Unless stated otherwise, all chemicals, reagents and solvents used in organic synthesis were purchased from Sigma-Aldrich (St. Louis, MO) and were used without any further purification. Fluoro-pyridin-3-amine was purchased from Matrix Scientific, Columbia, SC. $^1$H NMR spectra were recorded on a Varian INOVA 400 MHz spectrometer. Chemical shifts are reported in parts per million (δ) relative DMSO-$d_6$ (δ 2.50). Spin multiplicities are given as s (singlet), d (doublet), dd (doublet of doublets), t (triplet), and m (multiplet). Low resolution mass spectra were obtained on a 1946C Agilent MSD single quad mass spectrometer (Agilent Technologies, Inc., Santa Clara, CA) operating in a positive electrospray mode. Reactions were monitored by thin layer chromatography (TLC) using precoated silica gel-GHLF plates (0.25 mm thickness) (Analtech, Newark, N.J.). The plates were visualized by a UV lamp. 2-(1-(4-Chlorobenzoyl-5-methoxy-2-methyl-1*H*-indo-3-yl)-*N*-(phenethyl)acetamide (**1**) was synthesized as previously described (Kalgutkar et al., 2000b). Pooled human and rat liver microsomes and recombinant P450 isozymes were purchased from BD Gentest (Woburn, MA). Reduced NADPH, ketoconazole and quinidine were purchased from Sigma-Aldrich (St. Louis, MO).

**2-(1-(4-Chlorobenzoyl)-5-methoxy-2-methyl-1*H*-indol-3-yl)-*N*-(4-fluorophenyl)acetamide (2).** To a stirred solution of indomethacin (1.6 g, 4.5 mmol) in methylene chloride (20 ml) at room temperature were added oxalyl chloride (0.42 ml, 4.9 mmol) and anhydrous DMF (35 µl, 0.45 mmol). The mixture was stirred for 2 h at room temperature. 4-Fluoroaniline (990 mg, 9.0 mmol) was then added, and the mixture was stirred overnight at room temperature. The reaction mixture was diluted with water and methylene chloride. The organic layer was washed successively with 1.0 M aqueous hydrochloric acid solution, 1.0 M aqueous sodium hydroxide solution and brine. The organic layer was dried over anhydrous magnesium sulfate, filtered and concentrated *in vacuo*. The residue was triturated in *tert*-butyl methyl ether, which caused a white precipitate to form. The precipitate was filtered and washed with *tert*-butyl methyl ether. The precipitate was dried *in vacuo* to afford 1.4 g (70%) of **2** as a white solid. $^1$H NMR (DMSO-$d_6$) δ 10.23 (br s, 1H), 7.65 (d, 2H, $J$ = 8.0 Hz), 7.61 (d, 2H, $J$ = 8.0 Hz),

7.58 (dd, 2H, *J* = 8.0, 4.0 Hz), 7.14 (d, 1H, *J* = 4.0 Hz), 7.10 (t, 2H, *J* = 8.0 Hz), 6.89 (d, 1H, *J* = 8.0 Hz), 6.68 (dd, 1H, *J* = 8.0, 4.0 Hz), 3.71 (s, 3H), 3.70 (s, 2H), 2.24 (2, 3H); low resolution MS (ESI) *m/z* 450.9 [M + H].

**2-(1-(4-Chlorobenzoyl)-5-methoxy-2-methyl-1*H*-indol-3-yl)-*N*-(6-fluoropyridin-3-yl)acetamide (3)** was prepared from indomethacin (1.6 g, 4.5 mmol) and 6-fluoropyridin-3-amine (1.0 g, 9.0 mmol) in a manner similar to that described for the preparation of compound **2** in 60% yield (1.2 g). The title compound was isolated as a white solid. $^1$H NMR (DMSO-$d_6$) δ 10.48 (br s, 1H), 8.40 (m, 1H), 8.13 (m, 1H), 7.67 (d, 2H, *J* = 8.0 Hz), 7.62 (d, 2H, *J* = 8.0 Hz), 7.14 (d, 1H, *J* = 4.0 Hz), 7.12 (dd, 1H, *J* = 8.0, 4.0 Hz), 6.91 (d, 1H, *J* = 8.0 Hz), 6.69 (dd, 1H, *J* = 8.0, 4.0 Hz), 3.76 (s, 2H), 3.72 (s, 3H), 2.25 (s, 3H); low resolution MS (ESI) *m/z* 451.9 [M + H].

**2-(2-(1-(4-Chlorobenzoyl)-5-methoxy-2-methyl-1*H*-indol-3-yl)acetamido)acetic acid (4). Step 1. Preparation of *tert*-Butyl-2-(2-(1-(4-chlorobenzoyl)-5-methoxy-2-methyl-1*H*-indol-3-yl)acetamido)acetic acetate.** The *tert*-butylglycine amide derivative was synthesized from indomethacin (1.6 g, 4.5 mmol) and glycine *tert*-butyl ester (1.2 g, 9.0 mmol) via a similar procedure to that described for **2**. The compound was isolated as a white solid in 90% yield (1.9 g). $^1$H NMR (DMSO-$d_6$) δ 8.24 (t, 1H, *J* = 4.0 Hz), 7.65 (d, 2H, *J* = 8.0 Hz), 7.59 (d, 2H, *J* = 8.0 Hz), 7.08 (d, 1H, *J* 4.0 Hz), 6.90 (d, 1H, *J* = 8.0 Hz), 6.65 (dd, 1H, *J* = 8.0, 4.0 Hz), 3.72 (s, 3H), 3.67 (d, 2H, *J* = 4.0 Hz), 3.53 (s, 2H), 2.18 (s, 3H), 1.33 (s, 9H); low resolution MS (ESI) *m/z* 492.9 [M + Na]. **Step 2.** To a stirred solution of indomethacin-*tert*-butylglycine amide (1.0 g, 2.1 mmol) in methylene chloride (20 ml) was added trifluoroacetic acid (10 ml). The solution was stirred at room temperature for 1 h and then concentrated *in vacuo*. The remaining yellow residue was triturated in *tert*-butyl methyl ether to give a white precipitate. The precipitate was filtered and washed with *tert*-butyl methyl ether. The precipitate was dried *in vacuo* to afford 0.75 g (85%) of **4** as a white solid. $^1$H NMR (DMSO-$d_6$) δ 12.50 (br s, 1H), 8.25 (t, 1H, *J* = 4.0 Hz), 7.64 (d, 2H, *J* =8.0 Hz), 7.59 (d, 2H, *J* = 8.0 Hz), 7.09 (d,

DMD Fast Forward. Published on February 5, 2009 as DOI: 10.1124/dmd.108.026112
This article has not been copyedited and formatted. The final version may differ from this version.


1H, *J* = 4.0 Hz), 6.90 (d, 1H, *J* = 8.0 Hz, ), 6.65 (dd, 1H, *J* = 8.0, 4.0 Hz), 3.72 (s, 3H), 3.71 (d, 2H, *J* = 4.0 Hz), 3.52 (s, 2H), 2.17 (s, 3H); low resolution MS (ESI) *m/z* 414.9 [M + H].

**Modeling of Metabolism of Indomethacin and its Analogs.** All calculations were performed on a Windows Pentium personal computer. The software utilized in the computational analysis was *MetaSite* v. 2.8.7 (Molecular Discovery Ltd, http://moldiscovery.com). Two-dimensional structures of the compounds (generated in a simplified molecular input line entry system (SMILES) notation) were submitted to the *MetaSite* program, which is a fully automated procedure. The *MetaSite* version used in this analysis contains the homology 3D-models of P4501A2, P4502C9, P4502C19, P4502D6, and P4503A4 (Cruciani et al., 2005). *MetaSite* analyses to predict sites of metabolism involve the calculation of two sets of descriptors, one set of descriptors for P450 enzyme(s) and one for substrate. The resulting analysis provides a "chemical fingerprint" of the enzyme and the substrate. Chemical fingerprints are distance-based descriptors that are calculated from molecular interaction forces computed by GRID. *MetaSite* considers the chemical reactivity of the compound by taking into consideration the activation energy in the hydrogen abstraction step that ultimately generates metabolite(s). Hydrogen abstraction processes have been simulated by *ab initio* calculations of small fragments from drug-like substrates for human P450s and stored in *MetaSite*. When a fragment in the target molecule is recognized as one in the *MetaSite* database, all atoms in that fragment are assigned the corresponding reactivity value. The final ranking for potential metabolic sites is the product of the similarity analysis and the chemical reactivity. Once the structures of the compounds are provided, the semiempirical calculations, pharmacophore recognition, descriptor handling, similarity and reactivity computation are all carried automatically.

**Incubations with Liver Microsomes.** *Microsomal stability.* Stock solutions of test substrates were prepared in methanol. The final concentration of methanol in the incubation media was 0.2% (v/v). Half-life ($t_{1/2}$) assessments in microsomes were determined in duplicate after incubation of test substrates (1 μM) with rat or human liver microsomes (P450 concentration, 0.25 μM) in 0.1 M

DMD Fast Forward. Published on February 5, 2009 as DOI: 10.1124/dmd.108.026112
This article has not been copyedited and formatted. The final version may differ from this version.


potassium phosphate buffer (pH 7.4) at 37 °C. The total incubation volume was 0.6 ml. The reaction mixture was prewarmed at 37 °C for 2 min before adding NADPH (1.2 mM). Aliquots (75 µl) of the reaction mixture at 0, 5, 15, and 30 min (time period associated with reaction linearity) were added to acetonitrile (200 µl) containing diclofenac (0.05 µg/ml) as internal standard, and the samples were centrifuged at 2,500 x *g* for 5 min prior to liquid chromatography/tandem mass spectrometry (LC-MS/MS) analysis of substrate disappearance. For control experiments, NADPH and or liver microsomes were omitted from these incubations. To assess the involvement of P4503A4 and P4502D6 isoforms in the metabolism of indomethacin-amide derivatives, separate incubations were conducted wherein the P4503A4-specific inhibitor ketoconazole (1 µM) or the P4502D6 inhibitor quinidine (3 µM) were added to human liver microsomal incubations containing test substrate and NADPH and the stability reassessed in the presence of inhibitor.

*Metabolite identification.* For the purposes of metabolite identification studies, the concentration of test compound in the microsomal incubations was raised to 20 µM and that of P450 in rat and human liver microsomes was raised to 0.5 µM. The duration of the incubation time was increased from 30 min to 45 min. After quenching the incubation mixtures with 2 volumes of acetonitrile, the solutions were centrifuged (3,000 x *g*, 15 min) and the supernatants were dried under a steady nitrogen stream. The residue was reconstituted with mobile phase and analyzed for metabolite formation by LC/MS-MS.

***In Vivo* Studies.** Animal care and *in vivo* procedures were conducted according to guidelines of the Pfizer Animal Care and Use Committee. Jugular vein cannulated male Sprague-Dawley rats (230-250 g), obtained from Charles River Laboratories (Wilmington, MA) were used for these studies. All animals were housed individually. All animals were fasted overnight before dosing whereas access to water was provided *ad libitum*. Animals were fed following collection of the 4 h blood samples. Test compounds **1**-**4** were administered intravenously (iv) via the jugular vein of rats over 30 s at 1.0 mg/kg, respectively, and serial blood samples were collected before dosing and 0.083, 0.15, 0.5, 1, 2, 4, 6, 8 and 24 h after dosing. The vehicle used in intravenous administration was 95% glycerol formal

DMD Fast Forward. Published on February 5, 2009 as DOI: 10.1124/dmd.108.026112
This article has not been copyedited and formatted. The final version may differ from this version.


containing 5% DMSO. Test compounds **1-4** were also administered orally (po) at 5.0 mg/kg as solutions in PEG400. Blood samples were taken prior to po administration then serial samples were collected at 0.15, 0.5, 1, 2, 4, 6, 8 and 24 h after dosing. Blood samples from the various pharmacokinetic studies were centrifuged at 3000 rpm for 10 min at 4 °C to generate plasma. All plasma samples were kept frozen until analysis. Aliquots of plasma (100 μl) were transferred to 96-well blocks and acetonitrile (200 μl) containing diclofenac as internal standard (50 ng/ml) was added to each well. Samples were prepared for analysis by solid phase extraction using a Waters Oasis® MAX (10 mg) extraction plate (Waters Corp, MA, USA), following the manufacturers directions. Following extraction, the samples were then analyzed by LC-MS/MS and concentrations of analyte in plasma were determined by interpolation from a standard curve.

**Metabolite Identification Using Triple Quadrupole Linear Ion Trap LC-MS/MS.** The LC system consisted of Shimadzu LC20AD pumps, DGU20A5 degasser and VP Option box (Columbia, MD), an HTC PAL autosampler (Leap Technologies, Cary, NC), and a Phenomenex Luna C8(2) HPLC column (4.6 × 150 mm, 4 μm (Phenomenex, Torrance, CA)). LC mobile phase A was formic acid in water (0.1 %v/v), and mobile phase B was formic acid in acetonitrile (0.1%). The flow rate was 0.7 ml/min. The LC gradient started at 5% B for 5 min, ramped linearly to 90% B over 30 min, held at 90% B over 5 min, and then returned to the initial condition over 1.0 min. Post-column flow was split such that mobile phase was introduced into the mass spectrometer via an electrospray interface at a rate of 175 μl/min. The remaining flow was diverted to the PDA detector to provide simultaneous UV detection (λ= 254 nm) and total ion chromatogram. The LC system was interfaced to an API 4000 Q-trap mass spectrometer (Sciex, Toronto, Canada) equipped with the Turboionspray source. Metabolites were characterized in the full scan mode (from *m/z* 100 to 850) by multiple reaction monitoring (MRM)-enhanced product ion mode following preset MRM transitions derived from the collision-induced dissociation (CID) information and using precursor ion scans using the major common

DMD Fast Forward. Published on February 5, 2009 as DOI: 10.1124/dmd.108.026112
This article has not been copyedited and formatted. The final version may differ from this version.


fragment ion, m/z 139. Structural information was generated from the CID spectra of the corresponding protonated molecular ions.

**Analytical Methodology for Indomethacin Amides.** Substrate depletion in liver microsomal incubations as well as analyte concentrations in plasma samples were monitored on a Sciex API model 3000 LC/MS/MS triple quadrupole mass spectrometer. Analytes were chromatographically separated using a Hewlett Packard Series 1100 HPLC system. An autosampler was programmed to inject 20 µl on a Phenomenex Primesphere 5 µ C18-HC 30 x 2.0 mm column using a mobile phase consisting of 10 mM ammonium acetate buffer-acetonitrile (60:40 v/v) containing 0.2% (v/v) triethylamine and 0.1% (v/v) acetic acid at a flow rate varying from 1 to 1.5 ml/minute. Ionization was conducted in the positive ion mode at the ionspray interface temperature of 400 °C, using nitrogen for nebulizing and heating gas. The ion spray voltage was 5.0 kV and the orifice voltage was optimized at 30 eV. Substrates and internal standard were analyzed in the multiple reaction monitoring (MRM) mode. For test compounds, diagnostic transitions were obtained via separate studies involving direct infusion of the compounds into the mass spectrometer. For $t_{1/2}$ determinations in substrate depletion experiments in liver microsomes, substrate/internal standard peak height ratios were determined and normalized to the value obtained at time t = 0. The percentage of substrate remaining versus time was fitted to first-order decay functions to yield *in vitro* $t_{1/2}$ values. If the test substrate demonstrated nonlinearity on log percentage remaining versus time curves, only those initial time points wherein log-linearity was observed were used to determine $t_{1/2}$ values. In the case of plasma samples from pharmacokinetic studies, calibration curves were prepared by plotting the appropriate peak area ratios against the concentrations of analyte in plasma using 1/x weighting of analyte/internal standard peak height ratios. The concentration of the analytes in the plasma samples was determined by interpolation from the standard curve. The dynamic range of the assay was 5-2500 ng/ml.

**Pharmacokinetic Data Analysis.** Plasma concentration-time profiles were analyzed using the well-established non-compartmental method in WinNonLin v2.1 (Pharsight, Mountain View, CA). Plasma

DMD Fast Forward. Published on February 5, 2009 as DOI: 10.1124/dmd.108.026112
This article has not been copyedited and formatted. The final version may differ from this version.


clearance ($CL_p$) was calculated as the iv dose divided by the area under the plasma concentration-time curve from zero to infinity ($AUC_{0-\infty}$). $AUC_{0-\infty}$ was calculated by the linear trapezoid rule. The terminal slope of the ln(concentration) versus time plot was calculated by linear least-squares regression and the half-life was calculated as 0.693 divided by the absolute value of the slope. The steady state volume of distribution ($V_{dss}$) was determined using non-compartmental analysis as follows:

$$V_{dss} = (\text{iv dose x AUMC})/(\text{AUC})^2,$$

Where AUMC is the total area under the first moment of the drug concentration-time curve from time zero to infinity.

The relative bioavailability (*F*) of the po doses was calculated by using the following equation:

$$F = AUC_{0-\infty}{}^{po} / AUC_{0-\infty}{}^{iv} \text{ x } \text{Dose}^{iv} / \text{Dose}^{po}$$

**Results**

**Chemistry.** As depicted in Figure 3, well-established methodology was employed in the synthesis of the amide derivatives of indomethacin. Indomethacin amides **1**-**3** were prepared by treatment with the appropriate amine (or hydroxyl amine) derivatives utilizing oxalyl chloride as the carboxylic acid activator. Indomethacin-glycine analog **4** was synthesized in two steps via initial coupling of indomethacin with *tert*-butylglycine ester in the presence of oxalyl chloride followed by acid-catalyzed ester hydrolysis of the intermediate indomethacin-*tert*-butylglycine amide.

**Prediction of the Metabolic Fate of Indomethacin and Indomethacin-*N*-phenethylamide (1) by *MetaSite*.** The P4502C9 homology model in the software was used to predict indomethacin metabolites since the isozyme is principally responsible for oxidative metabolism of the NSAID (Nakajima et al., 1998). Metabolism prediction for **1** was restricted to P4503A4/P4502D6 given the role these isoforms play in the biotransformation of **1** (Remmel et al., 2004). The predictions for both compounds were executed without any input of information of known metabolites. As shown in Figure 1, *MetaSite* correctly predicted the P4502C9-catalyzed *O*-demethylation of indomethacin as the most likely biotransformation pathway. In the case of **1**, *MetaSite* predicted that P4503A4 and P4502D6-

DMD Fast Forward. Published on February 5, 2009 as DOI: 10.1124/dmd.108.026112
This article has not been copyedited and formatted. The final version may differ from this version.


mediated oxidations would principally occur on the phenethyl substituent (benzylic $CH_2$ and *para*-position on the phenyl ring); next in hierarchy was the prediction of *O*-demethylation by the two isozymes (see Figure 1). *MetaSite* prediction of benzylic oxidation by P4503A4 as the most plausible metabolic fate proved to be accurate since the principal metabolic fate of **1** in NADPH-supplemented human liver microsomes has been unambiguously shown to involve mono-hydroxylation on the benzylic carbon (metabolite **M1**) followed by further oxidation of this secondary alcohol metabolite to the ketone derivative **M2**. In addition to benzylic oxidation, *MetaSite* predicted *para*-aromatic hydroxylation on the phenethyl substituent as a very likely pathway. This prediction was incorrect since Remmel et al. (2004) have proven (using a synthetic standard of *para*-hydroxy-**1**) that **1** is not prone to aromatic ring hydroxylation. *Metasite* predicted that the possibility of oxidation on the carbon $\alpha$ to the amide nitrogen yielding **M3** and *O*-demethylation to **M4** was low and indeed this turned out to be the case. Interestingly, *MetaSite* indicated that *O*-demethylation in **1** to metabolite **M4** was likely to be catalyzed by both P4503A4 and P4502D6 but in reality this metabolic sequence occurs only via P4502D6 (Remmel et al., 2004). The metabolic profile of **1** in human liver microsomes is shown in Figure 4 and is similar to the one observed by Remmel et al. (2004).

**Prediction of the Metabolic Fate of Novel Indomethacin Amide Derivatives by *MetaSite*.** Considering that the *N*-linked substituent in **1** is most prone to oxidative metabolism by P4503A4, we designed virtual compounds **2**-**4** where we introduced electron-deficient (e.g., *N*-fluorophenyl and *N*-fluoropyridinyl) or polar (glycine derivative **4**) *N*-substituents to reduce oxidative metabolic liability in this region. In the case of the anilide analogs **2** and **3**, the electron-deficient fluorophenyl and fluoropyridinyl ring systems were also chosen to avoid reactive metabolite formation via aromatic hydroxylation *para* to the acetanilide nitrogen followed by two-electron oxidation to the electrophilic quinone-imine in a manner similar to that observed with acetaminophen (Dahlin et al., 1984). Upon presentation of compounds **2**-**4** to *MetaSite*, the prediction in each case shifted from metabolism on the *N*-substituent to *O*-demethylation as the most likely route of metabolism mediated by P4503A4 and

DMD Fast Forward. Published on February 5, 2009 as DOI: 10.1124/dmd.108.026112
This article has not been copyedited and formatted. The final version may differ from this version.


P4502D6 for compounds **2** and **3** and by P450 enzymes 3A4, 2D6 and 2C9 for carboxylic acid derivative **4** (Figure 2). Indeed, this was a fairly precise prediction since upon synthesis of **2**-**4** and testing for metabolism in NADPH-supplemented human liver microsomes, *O*-demethylation was observed as an almost exclusive pathway for the three compounds (Figures 5-8). As in the case with **1** (Remmel et al., 2004), indomethacin, a potential metabolite arising from amidase-mediated hydrolysis of compounds **2**-**4** was not observed in these incubations.

**Liver Microsomal Stability Assessments for Indomethacin-Amide Derivatives and Identification of P450 Isozymes Responsible for Metabolism.** The microsomal stability of indomethacin and its neutral amide derivatives (final concentration = 1 μM) was assessed by monitoring substrate consumption following incubation with human and rat liver microsomes in the presence of NADPH cofactor for 30 min at 37 °C (Table 1). Also shown in Table 1 are the physiochemical parameters (molecular weight and LogP) and the unbound fractions of the test compounds in rat plasma and rat liver microsomes that were predicted using *in silico* methodology described previously (Gao et al., 2008). Consistent with previous results (Remmel et al., 2004), indomethacin-*N*-phenethylamide (**1**) was highly unstable ($t_{1/2} \leq 2$ min) in rat and human liver microsomes supplemented with NADPH, whereas, amides **2** and **3** were relatively more stable as reflected by the longer $t_{1/2}$ values. Unbound fraction estimates in rat microsomes and plasma were comparable for the three neutral amides. In contrast, the glycine amide derivative **4** was devoid of metabolic turnover in both rat and human liver microsomes ($t_{1/2} > 90$ min). Under these experimental conditions, parent NSAID indomethacin was resistant to metabolic turnover ($t_{1/2} > 90$ min). Consistent with lower logP values, the fraction unbound for indomethacin and glycine amide derivative **4** in rat microsomes and plasma were higher than those predicted for the more lipohilic neutral amides **1**-**3**. Indomethacin amides **1**, **2**, and **3** were stable ($t_{1/2} > 90$ min) in incubations lacking NADPH or liver microsomes from rat and human. Substrate depletion experiments in human liver microsomes were also inducted in the presence of the P4503A4- and P4502D6-selective inhibitors ketoconazole and

DMD Fast Forward. Published on February 5, 2009 as DOI: 10.1124/dmd.108.026112
This article has not been copyedited and formatted. The final version may differ from this version.


quinidine, respectively. As shown in Table 2, co-incubation with ketoconazole rendered amides **1**, **2**, and **3** to be completely stable towards oxidation. Inclusion of quinidine had a less pronounced effect on metabolic turnover of indomethacin-amide derivatives. While, the P450 phenotyping using isozyme-specific inhibitors could not be conducted for **4** due to lack of substrate depletion in microsomes, separate studies using recombinant P4503A4, 2D6, and 2C9 isozymes revealed that only P4502C9 was capable of *O*-demethylating **4** (data not shown).

***In Vivo* Pharmacokinetics.** In order to evaluate whether the increased metabolic resistance of amides **2**, **3**, and **4** (as compared with **1**) translates into improvements in clearance and oral bioavailability, we decided to examine the pharmacokinetics of amides **1**-**4** following iv and po administration to Sprague-Dawley rats at 1 and 5 mg/kg, respectively. Table 3 summarizes the values (mean ± SD) of the pharmacokinetic parameters for **1**, **2**, **3**, and **4** after iv and po administration. Plasma concentrations after iv administration of indomethacin-*N*-phenethyl amide (**1**) declined very rapidly resulting in an estimated $CL_p$ value of 155 ± 41.5 ml/min/kg, which exceeded rat hepatic blood flow (70 ml/min/kg). In contrast, amide derivatives **2**, **3**, and **4** demonstrated significant attenuation in $CL_p$ values. Following po administration of **1**, systemic exposure at all sampling points was below the limit of detection (5 ng/ml). In contrast, oral dosing of amides **2**, **3**, and **4** led to measurable systemic exposure, which allowed estimation of the corresponding $C_{max}$ and $AUC_{0-\infty}$ values. The oral bioavailabilities of amides **2**, **3**, and **4** in the rat were 20, 38.5 and 37.6%, respectively.

## Discussion

Rather than using *MetaSite* to predict metabolism for a large number of structurally diverse substrates, our objective here was a focused analysis of a small subset of compounds within a given chemical series for the purposes of lead optimization. Comparison of the predictions for indomethacin and **1** with published experimental data showed a high degree of accuracy (>80% success rate), which is in good agreement with published prediction rates of *MetaSite* for a large number of heterogeneous substrates (Cruciani et al., 2005; Zhou et al., 2006; Caron et al., 2007). Encouraged by these

DMD Fast Forward. Published on February 5, 2009 as DOI: 10.1124/dmd.108.026112
This article has not been copyedited and formatted. The final version may differ from this version.


preliminary observations, we decided to test the accuracy of metabolite predictions for additional indomethacin amide derivatives for which no prior experimental knowledge on their metabolism was available. The overarching objective of this exercise was to evaluate whether the tool can be used in drug discovery to build metabolic resistance into metabolically labile compounds; a feature that could potentially translate in improvements into pharmacokinetic properties.

Given the knowledge that the metabolic instability of **1** was primarily derived from metabolism on the pendant phenethyl group, we selected virtual indomethacin analogs **2**, **3**, and **4** in which we resorted to introducing electron-deficient or polar amide substituents as standard tactics used in medicinal chemistry to build metabolic resistance around soft-spots. In the case of the anilide analogs **2** and **3**, the electron-deficient fluorophenyl and fluoropyridinyl ring systems were deliberately chosen to avoid the potential for acetaminophen-type bioactivation to electrophilic quinone-imine intermediates. When the structures were presented to *MetaSite*, the software predicted a metabolic shift and assigned *O*-demethylation as the highest priority site for oxidation, predictions that were fairly accurate as determined from experimental metabolite identification studies on these analogs. It is noteworthy to point out that the predictions were restricted to metabolism by certain P450 isozymes (P4503A4 and 2D6 for the neutral amides **1**, **2**, and **3** and P4502C9 specifically included for indomethacin and the glycine amide **4**) based on our input into the software. This was primarily based on the experimental observations that P450 isozymes 2C9 and 3A4/2D6 are involved in the metabolism of indomethacin and its phenethylamide derivative **1** based upon which we inferred (later confirmed) that P4503A4/2D6 would also play a key role in the metabolism of neutral amides **2** and **3**. Because glycine amide **4** possessed a carboxylic acid group, we inferred (later confirmed) that P4502C9 would play an exclusive role in the metabolism of this anionic compound as per the norm with many P4502C9 substrates (Lewis et al., 2002). In addition, it is of interest to note that *MetaSite* predictions are not quantitative in nature. Based on chemical reactivity, the software assigns hierarchy (major vs. minor) to likely sites of metabolism, but does not provide insights into the overall metabolic stability of the molecule as it

DMD Fast Forward. Published on February 5, 2009 as DOI: 10.1124/dmd.108.026112
This article has not been copyedited and formatted. The final version may differ from this version.


relates to *in vitro* $t_{1/2}$ values and ultimately *in vivo* clearance. Evaluation of these latter attributes requires additional experimentation as was the case in our investigations wherein rat and human liver microsomal stability and rat pharmacokinetic data on amides **2**, **3**, and **4** had to be generated. Compared with **1**, neutral amides **2** and **3** were relatively more stable in NADPH-supplemented rat and human liver microsomes. In contrast, indomethacin and the glycine amide **4**, which contained free carboxylic acid substituents, were completely resistant to metabolism in liver microsomes from both species. Considering that microsomal unbound fractions of amides **1**, **2** and **3** predicted from *in silico* computational models (Gao et al., 2008) were comparable (Table 1), the free intrinsic clearance values (amide **1**: 6646 ml/min/kg, amide **2**: 2034 ml/min/kg, amide **3**: 772 ml/min/kg) obtained from scale-up of half-life data (normalized for non-specific microsomal binding) (Obach, 1999), suggested that the strategy of attenuating metabolism via structural modification of the amide substituent in **1** had worked in our favor. Of much interest in this endeavor were the observations on the similarity in metabolic stability and free microsomal fraction of indomethacin and glycine amide **4** that resulted in comparable intrinsic clearance predictions of < 10 ml/min/kg. The higher free fractions of indomethacin and glycine amide **4** in microsomes and plasma relative to the neutral amides **1** – **3** were anticipated given their lower lipophilicity values.

As the next step in our exercise, we were interested in seeing whether the decreases in free intrinsic clearance values half-lives of amides **2**-**4** in liver microsomes translated into a lower clearance and greater oral bioavailability in the rat. In contrast with the hepatic blood flow limited clearance observed with **1**, neutral indomethacin-amides **2** and **3** revealed moderate clearances in the range of 26-39 ml/min/kg. The possibility that higher plasma protein binding of amides **2** and **3** (compared with **1**) played a role in the diminished clearance can be ruled out given that the predicted unbound fraction of the neutral compounds in rat plasma is comparable (Table 1). Assuming that hepatic oxidative metabolism by P450 plays a major role in elimination, the clearance values for **2** and **3** will translate into hepatic extraction ratios of 0.37 to 0.55 (based on a rat hepatic blood flow of 70 ml/min/kg),

respectively, and could result in maximum possible oral bioavailability ranging from 45-63%. The observed lower oral bioavailability for **2** (F = 20 %) and **3** (F = 38.5 %) suggests that solubility and/or gut extraction could play a role in limiting oral absorption for these compounds in the rat. The observed *in vivo* clearance and oral bioavailability of the glycinyl amide **4** was comparable to that estimated for the fluorophenyl- and fluoropyridinyl amide derivatives **2** and **3**, respectively, despite free intrinsic clearance and plasma protein binding values comparable with the parent NSAID indomethacin. While not tested directly, plausible reason(s) for the in vitro–in vivo disconnect with **4** could be the existence of non-P450 clearance mechanism(s) such as phase II acyl glucuronidation and/or non-metabolic elimination pathway such as organic anion transporter-mediated renal excretion in a manner similar to that discerned with indomethacin and most other carboxylic acid-containing NSAIDs (Kouzuki et al., 2000; Sabolovic et al., 2000; Apiwattanakul et al., 1999). With respect to the higher *in vivo* clearance when compared with indomethacin, it is possible that **4** possesses a significantly greater affinity for glucuronidation enzymes and/or organic anion transporters than the parent NSAID.

Often times, chemical intervention strategies to optimize metabolic stability via modulation of physiochemical properties or soft spot blocking tactics can have an adverse effect on primary pharmacology resulting in loss of potency against biological target or shift in isozyme/receptor subtype selectivity. In the present investigation, this phenomenon becomes evident with the glycinyl amide derivative **4**. Unlike the phenethylamide derivative **1**, compound **4** is stable to degradation in rat and human microsomes indicative of a significant improvement in metabolic stability. However, this advantage is offset by the fact that unlike **1**, **4** is not a selective COX-2 inhibitor; in fact the compound does not inhibit the activities of either COX enzymes ($IC_{50}$ > 10 μM) (Bartolini W et al., patent application, WO 2007/070892 A2). In contrast, the neutral 4-fluorophenylamide derivative of indomethacin **2** has been reported to maintain the potent and selective COX-2 inhibitory attributes of **1** (phenethylamide (**1**): COX-2 $IC_{50}$ = 0.066 μM; COX-1 $IC_{50}$ > 66 μM; 4-fluorophenylamide (**2**): COX-2

$IC_{50}$ = 0.066 μM; COX-1 $IC_{50}$ > 66 μM) (Kalgutkar et al., 2000b). Likewise, a close-in analog of the 4-fluoropyridinyl amide derivative **3**, in which the fluorine is replaced with a chlorine atom has been synthesized and shown to retain COX-2 potency and selectivity discerned with **1** (Kalgutkar et al., 2000b) suggesting that **3** would possess similar characteristics. Taken together, amides **2** and **3** represent a significant advantage over **1** in that they retain the primary pharmacology of **1** while offering a pharmacokinetic benefit due to improved metabolic stability.

In conclusion, *MetaSite* has not been designed to predict rates of oxidation ($V_{max}$ and $K_m$) or to provide quantitative predictions and furthermore its use is restricted to the major human P450 isozymes and their oxidative capacity. Nevertheless, as demonstrated in previous studies and this work, the *MetaSite* methodology is automated, rapid, and has relatively accurate predictions; consequently it can be used as a metabolic site prediction tool at the early drug discovery stage in terms of both speed and accuracy. However, it is best to confirm the predictions with experimental data for a few compounds within a chemical series to ensure preciseness of the predictions. In addition, it is noteworthy to point out that the problem explored in our study was of relatively low complexity considering that the lead compounds possessed few metabolic soft spots. Consequently, the accuracy of *MetaSite* in predicting metabolism of complex molecules (with numerous options for metabolism) needs to be examined further. Finally, during the course of this investigation, we also realized that the integration of *MetaSite* predictions and experimental data, interpretation of the similarities and differences in metabolism, *apriori* knowledge on the P450 isozymes involved in metabolism, etc, critically depends on the human expert.

DMD Fast Forward. Published on February 5, 2009 as DOI: 10.1124/dmd.108.026112
This article has not been copyedited and formatted. The final version may differ from this version.


## References

Ahlstrom MM, Ridderstrom M, Zamora I and Luthman K (2007) CYP2C9 structure-metabolism relationships: optimizing the metabolic stability of COX-2 inhibitors. *J Med Chem* **50:**4444-4452.

Apiwattanakul N, Sekine T, Chairoungdua A, Kanai Y, Nakajima N, Sophasan S and Endou H (1999) Transport properties of nonsteroidal anti-inflammatory drugs by organic anion transporter 1 expressed in Xenopus laevis oocytes. *Mol Pharmacol* **55:**847-854.

Caron G, Ermondi G and Testa B (2007) Predicting the oxidative metabolism of statins. An application of the *MetaSite*® algorithm. *Pharm Res* **24:**480-501.

Cruciani G, Carosati E, De Boeck B, Ethirajulu K, Mackie C, Howe T and Vianello R (2005) MetaSite: understanding metabolism in human cytochromes from the perspective of the chemist. *J Med Chem* **48:**6970-6979.

Dahlin DC, Miwa GT, Lu AY and Nelson SD (1984) N-acetyl-p-benzoquinone imine: a cytochrome P-450-mediated oxidation product of acetaminophen. *Proc Natl Acad Sci USA* **81:**1327-1331.

Dawidowicz AL, Kobielski M and Pieniadz J (2008) Anomalous relationship between free drug fraction and its total concentration in drug-protein systems II. Binding of different ligands to plasma proteins. *Eur J Pharm Sci* **35:**136-141.

Gao H, Yao L, Mathieu HW, Zhang Y, Maurer TS, Troutman MD, Scott DO, Ruggeri RB and Lin J (2008) In silico modeling of nonspecific binding to human liver microsomes. *Drug Metab Dispos* **36:**2130-2135.

Kalgutkar AS, Crews BC, Rowlinson SW, Marnett AB, Kozak KR, Remmel RP and Marnett LJ (2000a) Biochemically based design of cyclooxygenase-2 (COX-2) inhibitors: facile conversion of nonsteroidal antiinflammatory drugs to potent and highly selective COX-2 inhibitors. *Proc Natl Acad Sci USA* **97:**925–930.

Kalgutkar AS, Marnett AB, Crews BC, Remmel RP and Marnett LJ (2000b) Ester and amide derivatives of the nonsteroidal antiinflammatory drug, indomethacin, as selective cyclooxygenase-2 inhibitors. *J Med Chem* **43:**2860-2870.

Kouzuki H, Suzuki H and Sugiyama Y (2000) Pharmacokinetic study of the hepatobiliary transport of indomethacin. *Pharm Res* **17:**432-438.

Lewis DF, Modi S and Dickins M (2002) Structure-activity relationship for human cytochrome P450 substrates and inhibitors. *Drug Metab Rev* **34:**69-82.

Nakajima M, Inoue T, Shimada N, Tokudome S, Yamamoto T and Kuroiwa Y (1998) Cytochrome P450 2C9 catalyzes indomethacin O-demethylation in human liver microsomes. *Drug Metab Dispos* **26:**261-266.

Obach RS (1999) Prediction of human clearance of twenty-nine drugs from hepatic microsomal intrinsic clearance data: An examination of in vitro half-life approach and nonspecific binding to microsomes. *Drug Metab Dispos* **27:**1350-1359.

Obach RS, Kalgutkar AS, Soglia JR and Zhao SX (2008) In vitro metabolism and covalent binding of enol-carboxamide derivatives and anti-inflammatory agents sudoxicam and meloxicam: insights into the hepatotoxicity of sudoxicam. *Chem Res Toxicol* **21:**1890-1899.

Paine SW, Parker AJ, Gardiner P, Webborn PHJ and Riley RJ (2008) Prediction of the pharmacokinetics of atorvastatin, cerivastatin and indomethacin using kinetic models applied to isolated rat hepatocytes. *Drug Metab Dispos* **36:**1365-1374.

Remmel RP, Crews BC, Kozak KR, Kalgutkar AS and Marnett LJ (2004) Studies on the metabolism of the novel, selective cyclooxygenase-2 inhibitor indomethacin phenethylamide in rat, mouse, and human liver microsomes: identification of active metabolites. *Drug Metab Dispos* **32:**113-122.

Sabolovic N, Magdalou J, Netter P and Abid A (2000) Nonsteroidal anti-inflammatory drugs and phenols glucuronidation in Caco-2 cells: identification of the UDP-glucuronosyltransferases UGT1A6, 1A3 and 2B7. *Life Sci* **67:**185-196.

Zamora I, Afzelius L and Cruciani G (2003) Predicting drug metabolism: a site of metabolism prediction tool applied to the cytochrome P450 2C9. *J Med Chem* **46:**2313-2324.

Zhou D, Afzelius L, Grimm SW, Andersson TB, Zauhar RJ and Zamora I (2006) Comparison of methods for the prediction of the metabolic sites for CYP3A4-mediated metabolic reactions. *Drug Metab Dispos* **34:**976-983.

DMD Fast Forward. Published on February 5, 2009 as DOI: 10.1124/dmd.108.026112
This article has not been copyedited and formatted. The final version may differ from this version.


## Figure Legends

FIG. 1. Plots of *MetaSite* predictions for sites of metabolism for indomethacin and 2-(1-(4-chlorobenzoyl)-5-methoxy-2-methyl-1*H*-indol-3-yl]-*N*-phenethyl-acetamide (**1**). The functional groups in both compounds that most likely will be metabolized are marked; the darker the color the higher is the probability of metabolism to occur. Since oxidative metabolism (*O*-demethylation) of indomethacin is exclusively metabolized by P4502C9 (Nakajima et al., 1998), *in silico* predictions were only made with P4502C9. Likewise, since P4503A4 and P4502D6 are involved in the metabolism of **1**, we chose the software's ability to predict contributions from these two P450 isozymes.

FIG. 2. Plots of *MetaSite* predictions for sites of metabolism of neutral indomethacin-amide derivatives. The functional groups in both compounds that most likely will be metabolized are marked; the darker the color the higher is the probability of metabolism to occur. Based on the available P450 phenotyping information for **1**, we chose the software's ability to predict metabolism by P4503A4 and P4502D6 for compounds **2** and **3** and P4503A4, 2D6, and 2C9 for compound **4**. This *in silico* data was generated in a virtual fashion (i.e., prior to the actual synthesis of the compounds).

FIG. 3. Chemical preparation of the indomethacin-amides used in the studies.

FIG. 4. LC-MS/MS analysis of an incubation mixture containing indomethacin-*N*-phenethyl amide (**1**) (20 μM) and NADPH-supplemented human liver microsomes. The structures of metabolites **M1**-**M4** is also depicted; these metabolites were also observed by Remmel et al. (2004) in a independent metabolism study on **1**.

FIG. 5. LC-MS/MS analysis of an incubation mixture containing indomethacin-4-fluorophenyl amide (**2**), indomethacin-4-fluoropyridinyl amide (**3**), and indomethacin-glycine amide (**4**) (20 μM each) and NADPH-supplemented human liver microsomes.

DMD Fast Forward. Published on February 5, 2009 as DOI: 10.1124/dmd.108.026112
This article has not been copyedited and formatted. The final version may differ from this version.


FIG. 6. CID spectrum of indomethacin-4-fluorophenyl amide (**2**) (Panel A) and its *O*-demethylated metabolite (Panel B).

FIG. 7. CID spectrum of indomethacin-4-fluoropyridinyl amide (**3**) (Panel A) and its *O*-demethylated metabolite (Panel B).

FIG. 8. CID spectrum of indomethacin-glycine amide (**4**) (Panel A) and its *O*-demethylated metabolite (Panel B).

DMD Fast Forward. Published on February 5, 2009 as DOI: 10.1124/dmd.108.026112
This article has not been copyedited and formatted. The final version may differ from this version.


TABLE 1

*Rat and human liver microsomal stability of indomethacin and its amide derivatives **1-4***

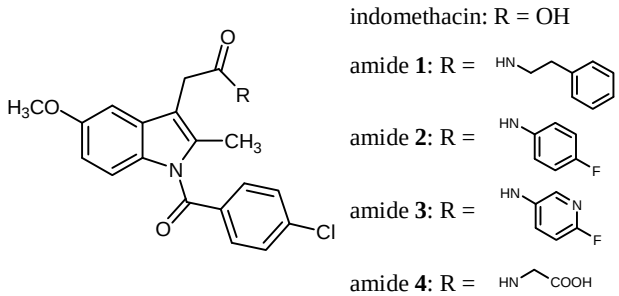


| Compound | MW / LogP[a] | Fraction Unbound[b] | $T_{1/2}$ (min) | |
|---|---|---|---|---|
| | | Rat plasma/microsomes | Rat | Human |
| Indomethacin | 357 / 4.18 | 0.030 / 0.91[c] | > 90 | > 90 |
| Amide **1** | 460 / 5.50 | 0.0045 / 0.13 | 1.0 | 1.5 |
| Amide **2** | 450 / 5.85 | 0.0040 / 0.05 | 8.5 | 25 |
| Amide **3** | 451 / 5.05 | 0.0070 / 0.14 | 8.0 | 23 |
| Amide **4** | 414 / 3.54 | 0.030 / 0.93 | >90 | > 90 |

[a]LogP values were calculated using the ACD software (Advanced Chemical Development, Inc.). [b]Fraction unbound estimates in rat plasma and rat liver microsomes were obtained using *in silico* models developed in Pfizer as previously described with human liver microsomes (Gao et al., 2008). Literature free fraction of indomethacin in rat plasma is 0.040 (Dawidowicz et al., 2008) indicating high confidence in the *in silico* predictions.

DMD Fast Forward. Published on February 5, 2009 as DOI: 10.1124/dmd.108.026112
This article has not been copyedited and formatted. The final version may differ from this version.


TABLE 2

*P450 isozymes responsible for metabolic turnover of indomethacin amides **1**-**3** in human liver microsomes*

| Compound | % Inhibition of substrate depletion | |
|---|---|---|
| | Microsomes + ketoconazole | Microsomes + Quinidine |
| Amide **1** | 96 | < 5 |
| Amide **2** | 100 | 35 |
| Amide **3** | 100 | 28 |

Indomethacin amide **4** was not tested since it was resistant to metabolic turnover.

Table 3

*Pharmacokinetic parameters of Indomethacin-amides **1-4** in male sprague-dawley rats*

| Compound | Dose (mg/kg) | Route | $C_{max}$ (ng/ml) | $T_{max}$ (h) | $CL_p$ (ml/min/kg) | $Vd_{ss}$ (l/kg) | $AUC_{0-\infty}$ (ng.h/ml) | $T_{1/2}$ (h) | F (%) |
|---|---|---|---|---|---|---|---|---|---|
| Amide **1** | 1.0 | iv | | | 155 ± 41.5 | 5.3 ± 1.2 | 114 ± 35.0 | 0.6 ± 0.1 | |
| | 5.0 | po | N.C.[a] | N.C.[a] | | | N.C.[a] | | N.C.[a] |
| Amide **2** | 1.0 | iv | | | 26.0 ± 9.40 | 2.3 ± 1.1 | 699 ± 240 | 1.1 ± 0.3 | |
| | 5.0 | po[b] | 57.0 | 3.0 | | | 677 | | 20 |
| Amide **3** | 1.0 | iv | | | 39.2 ± 4.50 | 2.0 ± 0.4 | 430 ± 49.0 | 1.0 ± 0.3 | |
| | 5.0 | po | 120 ± 55.8 | 1.2 ± 0.7 | | | 828 ± 490 | | 38.5 |
| Amide **4** | 1.0 | iv | | | 31.0 ± 7.00 | 0.7 ± 0.2 | 562 ± 150 | 1.4 ± 0.4 | |
| | 5.0 | po | 154 ± 42.1 | 1.0 ± 0.8 | | | 1060 ± 167 | | 37.6 |
| Indomethacin[c] | 1.0 | iv | | | 0.51 ± 0.04 | 0.19 ± 0.03 | | 4.6 ± 1.0 | |

Compounds were administered via iv bolus to fasted male Sprague-Dawley rats (N=3) in 95% glycerol formal containing 5% DMSO. For po studies, compounds were administered via gavage to fasted male Sprague-Dawley rats (N=3) as a suspension in 0.5% methyl cellulose. [a]N.C., not calculated (systemic exposure below the lower limit of quantitation (5 ng/ml)). [b]N=2 rats. [c]Intravenous pharmacokinetic data from Paine et al. 2008.

# Figure 1

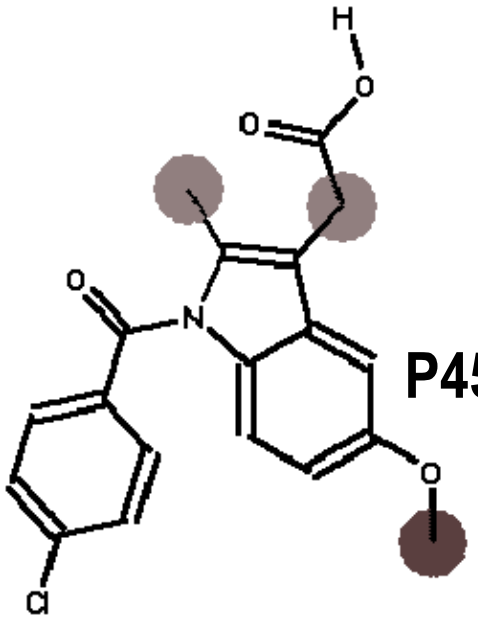

**P4502C9**

**Indomethacin** (MW = 357)
cLogP ~ 4.18

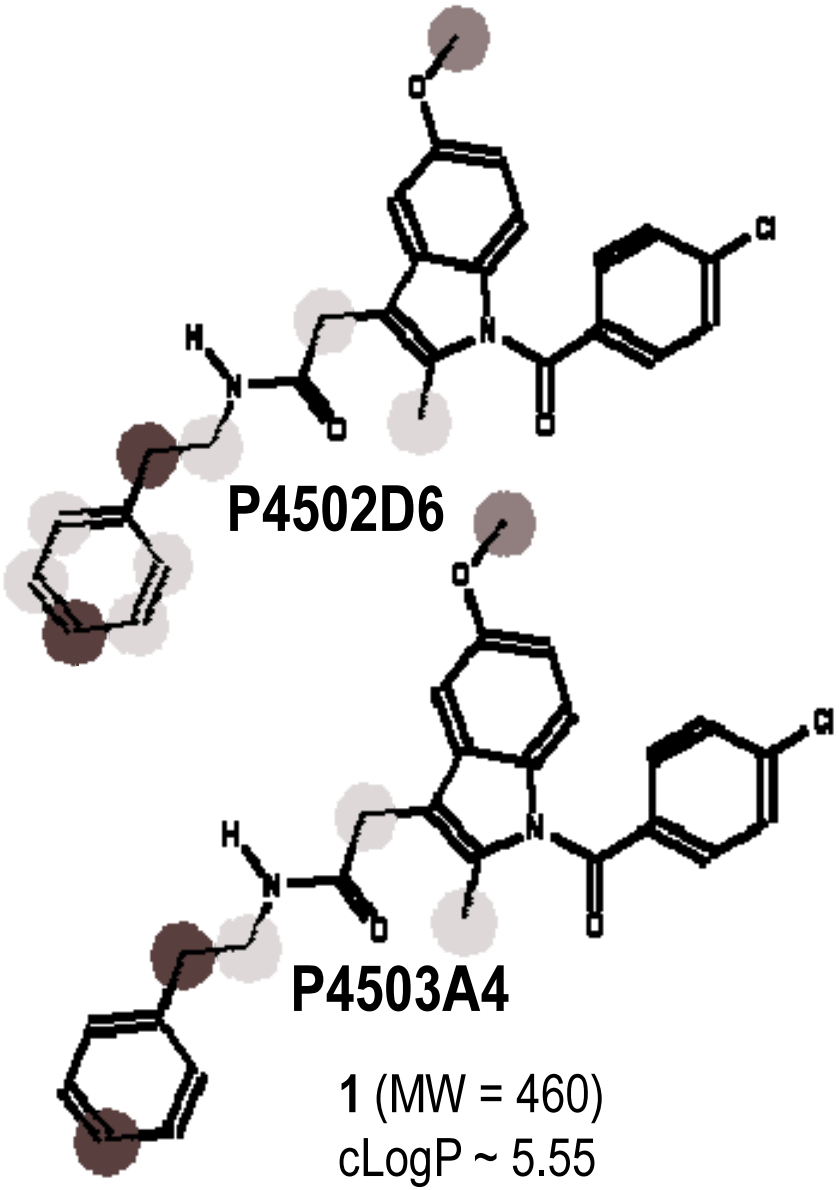

**P4502D6**

**P4503A4**

**1** (MW = 460)
cLogP ~ 5.55

# Figure 2

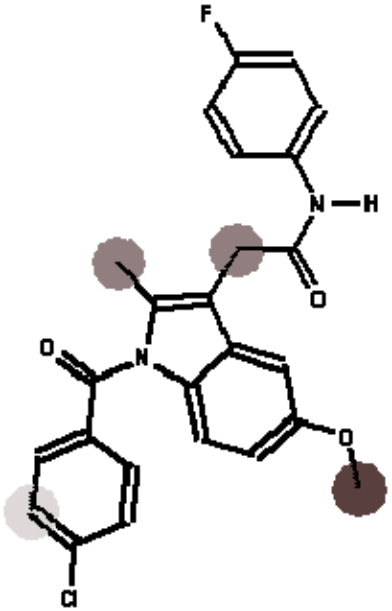

**P4502D6** **2** (MW = 450)
**P4503A4** cLogP ~ 5.86

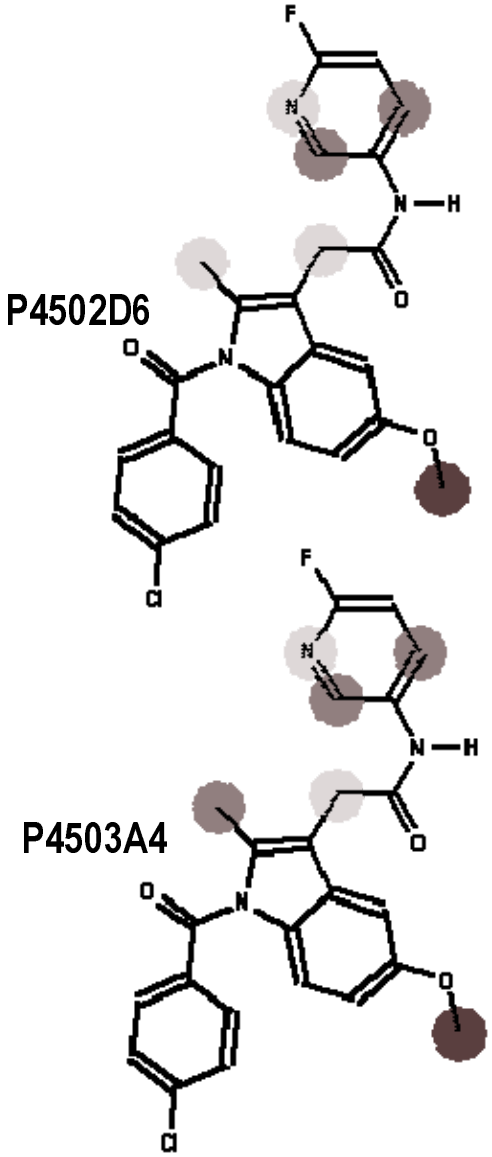


**3** (MW = 451)
cLogP ~ 5.05

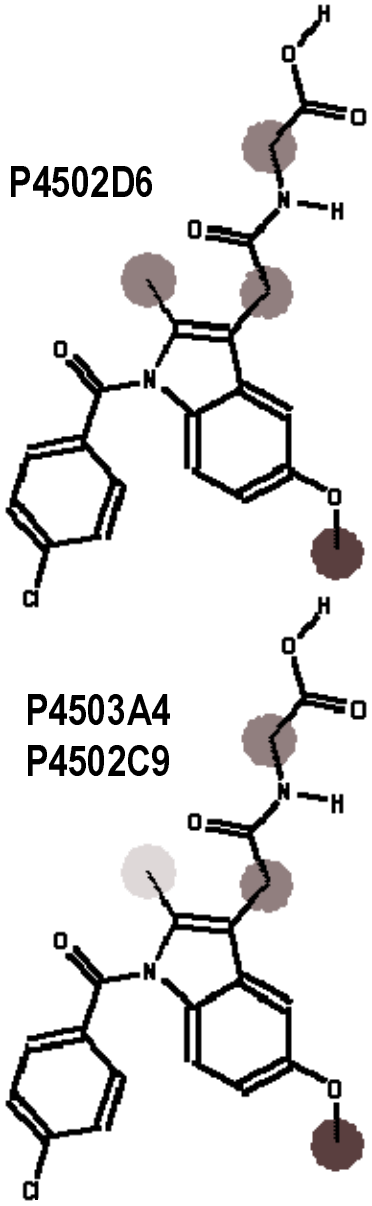


**4** (MW = 414)
cLogP ~ 3.54

# Figure 3

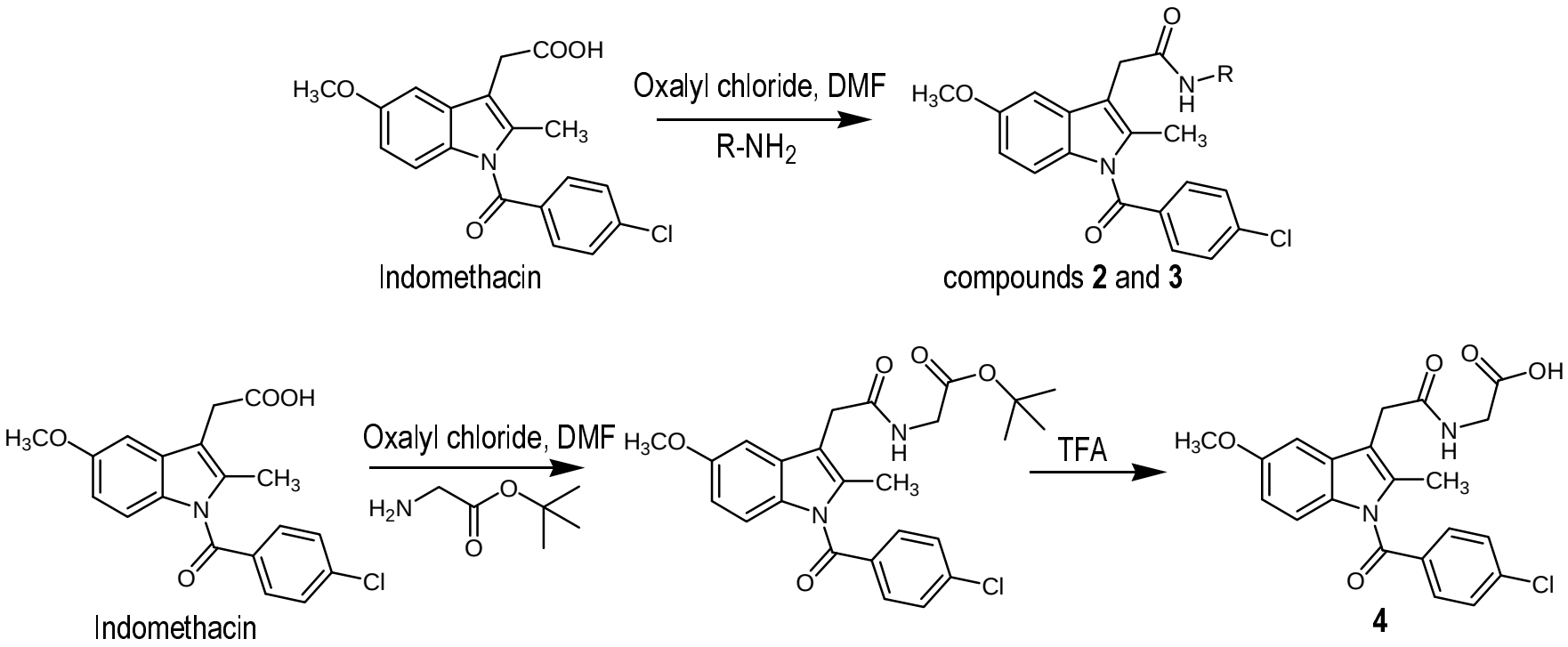

# Figure 4

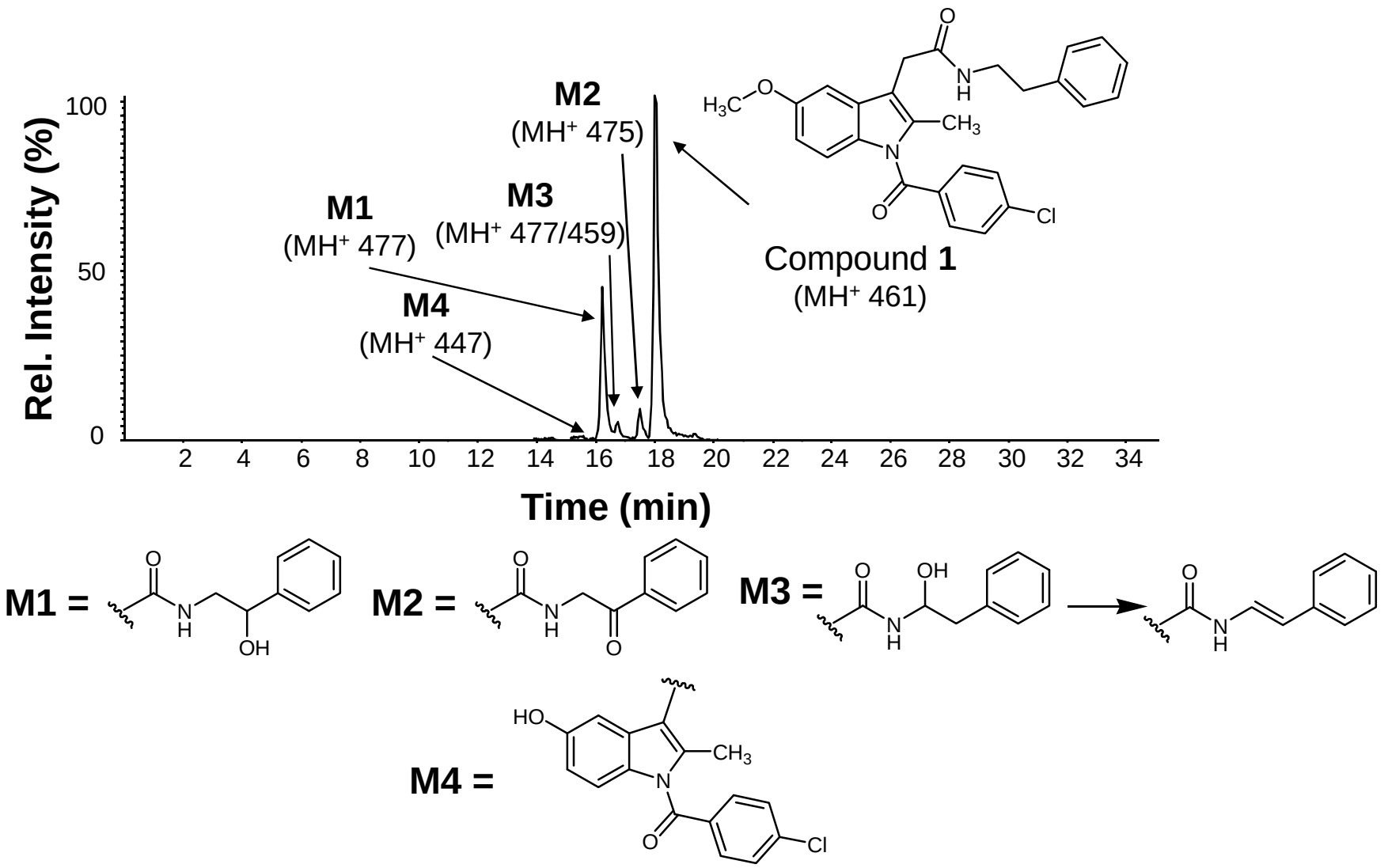

**Figure 5**

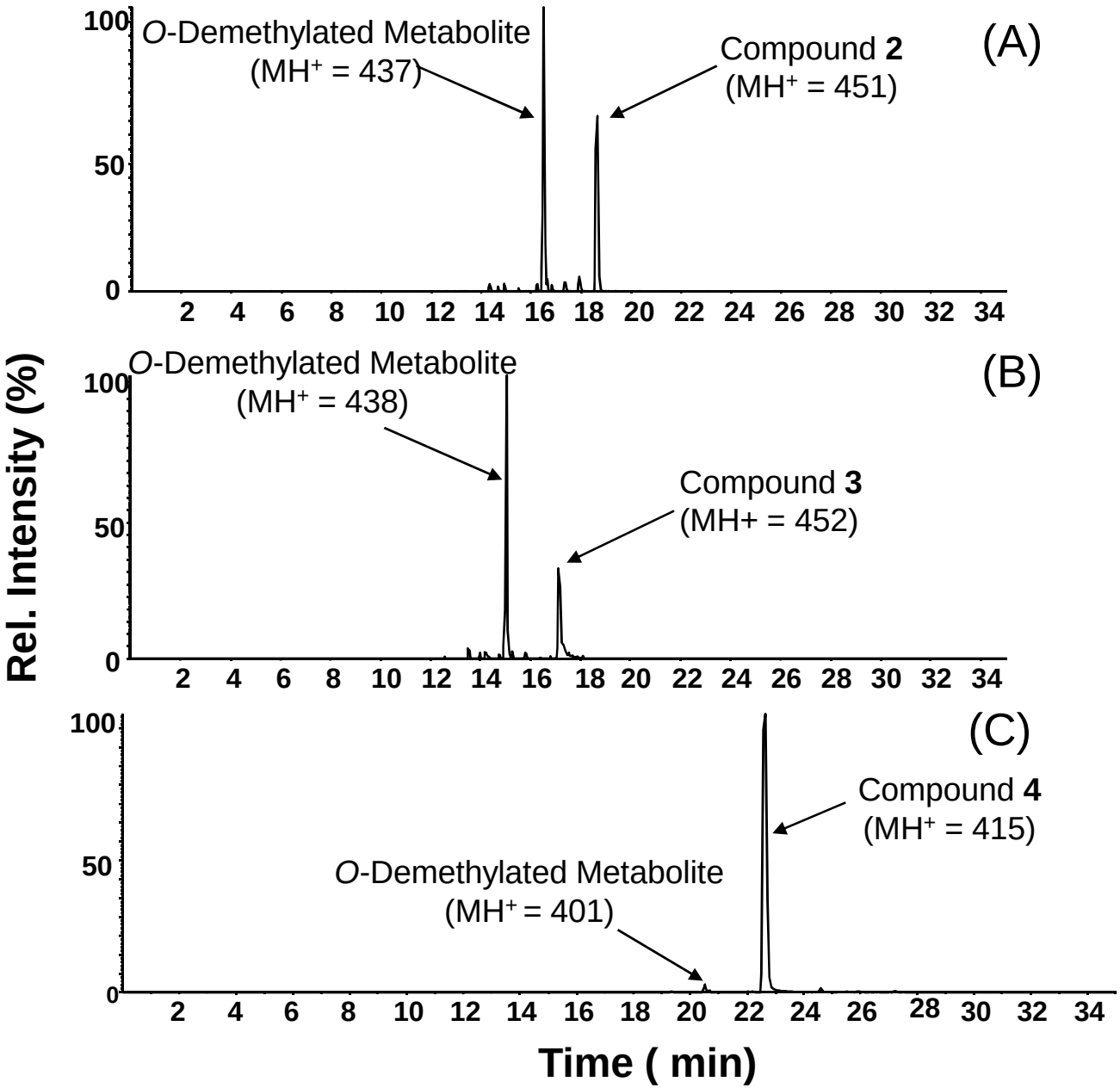

**Figure 6**

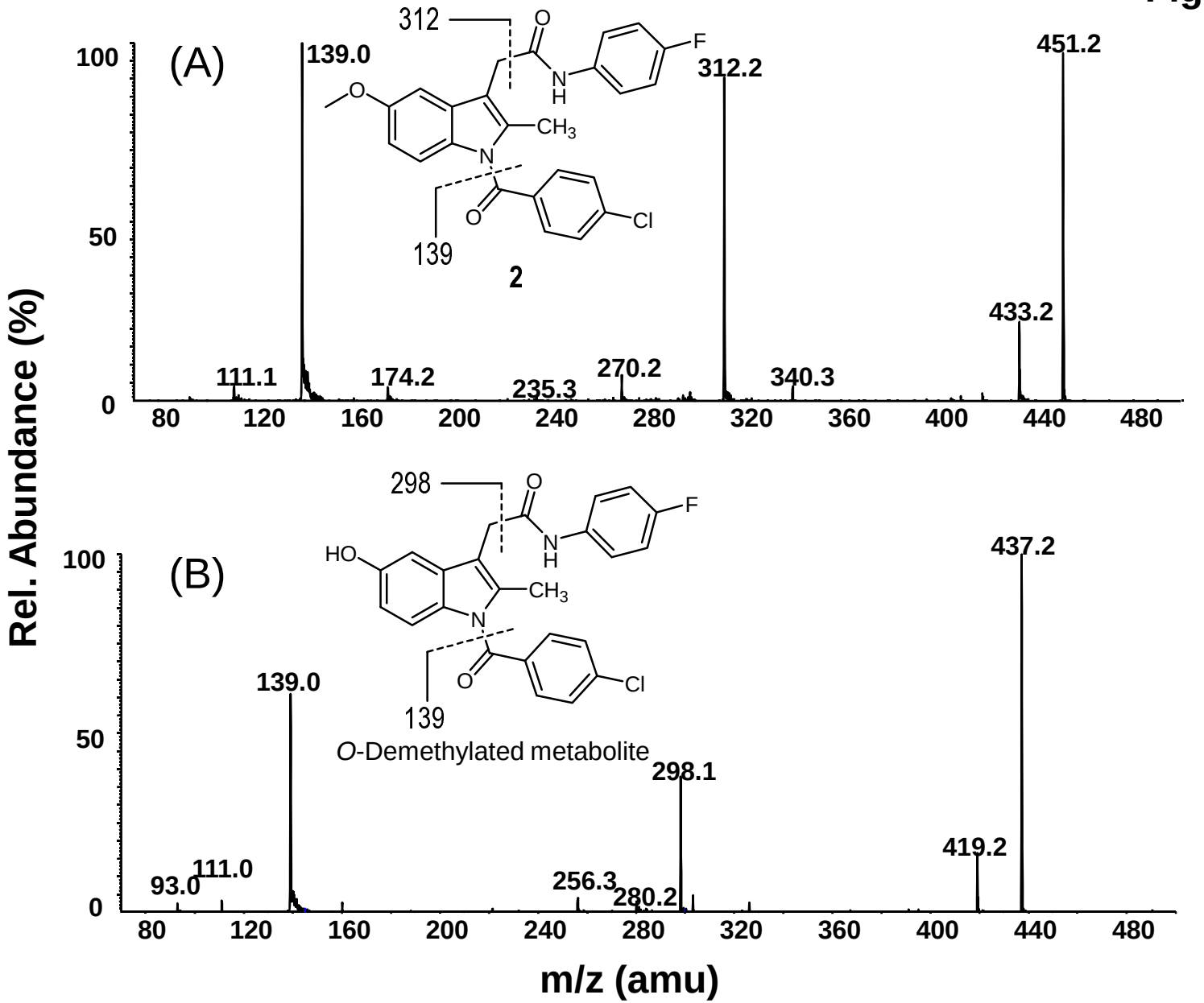

**Figure 7**

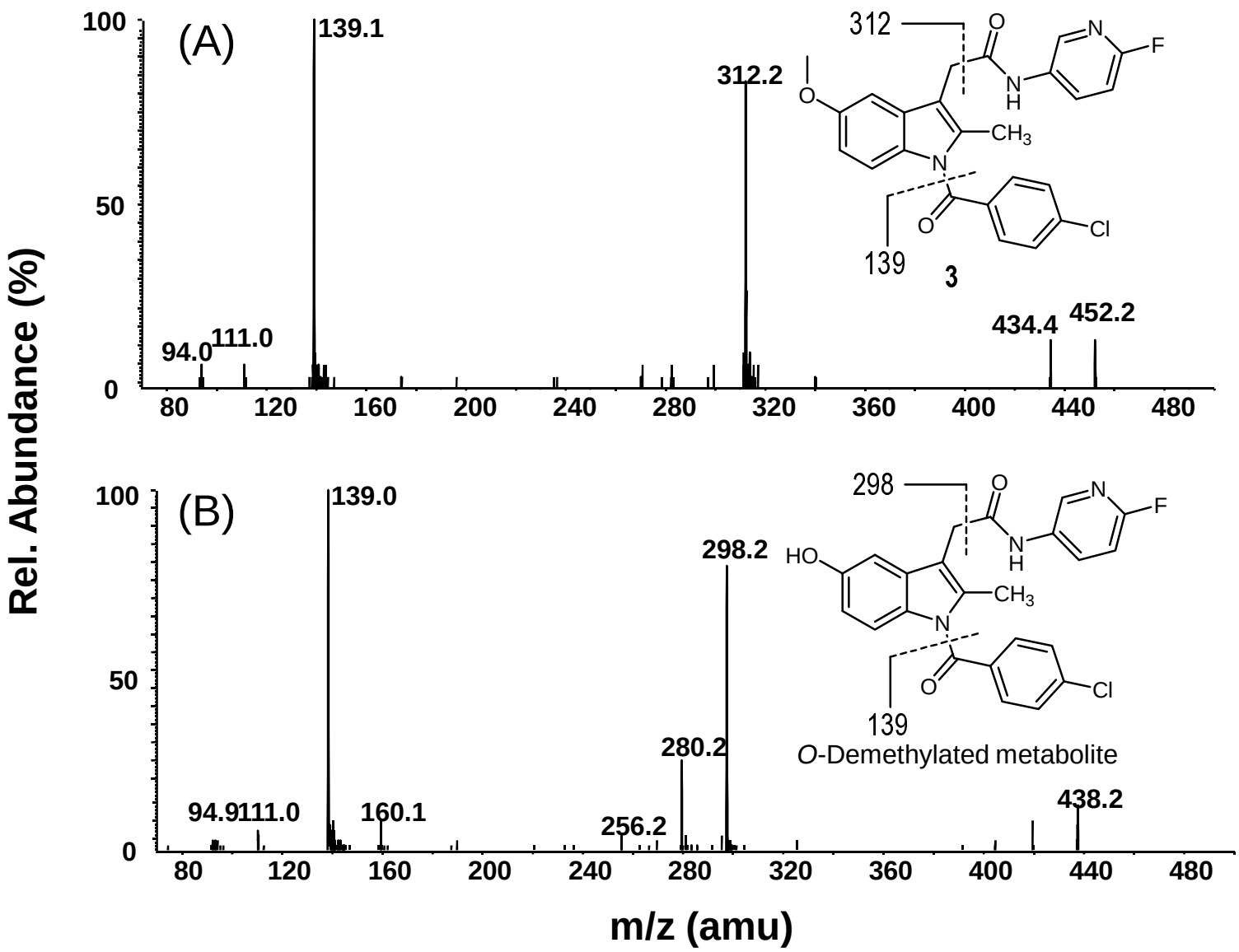

**Figure 8**